Yang *et al. Intell Robot* 2024;4(1):107-24
DOI: 10.20517/ir.2024.07

Intelligence & Robotics

Research Article

Open Access

Coordinated energy-efficient walking assistance for paraplegic patients by using the exoskeleton-walker system

Chen Yang, Xinhao Zhang, Long Zhang, Chaobin Zou, Zhinan Peng, Rui Huang, Hong Cheng

School of Automation Engineering, University of Electronic Science and Technology of China, Chengdu 611731, Sichuan, China.

Correspondence to: Dr. Chaobin Zou, School of Automation Engineering, University of Electronic Science and Technology of China, No. 2006, Xiyuan Ave, West Hi-Tech Zone, Chengdu 611731, Sichuan, China. E-mail: chaobinzou@uestc.edu.cn

How to cite this article: Yang C, Zhang X, Zhang L, Zou C, Peng Z, Huang R, Cheng H. Coordinated energy-efficient walking assistance for paraplegic patients by using the exoskeleton-walker system. *Intell Robot* 2024;4(1):107-24. http://dx.doi.org/10.20517/ir.2024.07

Received: 1 Dec 2023 **First Decision:** 16 Jan 2024 **Revised:** 7 Feb 2024 **Accepted:** 4 Mar 2024 **Published:** 19 Mar 2024

Academic Editor: Simon X. Yang **Copy Editor:** Dong-Li Li **Production Editor:** Dong-Li Li

Abstract

Overground walking can be achieved for patients with gait impairments by using the lower limb exoskeleton robots. Since it is a challenge to keep balance for patients with insufficient upper body strength, a robotic walker is necessary to assist with the walking balance. However, since the walking pattern varies over time, controlling the robotic walker to follow the walking of the human-exoskeleton system in coordination is a critical issue. Inappropriate control strategy leads to the unnecessary energy cost of the human-exoskeleton-walker (HEW) system and also results in the bad coordination between the human-exoskeleton system and the robotic walker. In this paper, we proposed a Coordinated Energy-Efficient Control (CEEC) approach for the HEW system, which is based on the extremum seeking control algorithm and the coordinated motion planning strategy. First, the extremum seeking control algorithm is used to find the optimal supporting force of the support joint in real time to maximize the energy efficiency of the human-exoskeleton system. Second, the appropriate reference joint angles for wheels of the robotic walker can be generated by the coordinated motion planning strategy, causing the good coordination between the human-exoskeleton system and the robotic walker. The proposed approach has been tested on the HEW simulation model, and the experimental results indicate that the coordinated energy-efficient walking can be achieved with the proposed approach, which is increased by 60.16% compared to the conventional passive robotic walker.

Keywords: Exoskeleton robots, robotic walker, energy efficiency, coordinated motion planning

1. INTRODUCTION

Overground walking is necessary and important for patients with gait impairments, which can be implemented using the lower limb exoskeleton robots. Usually, it is hard for patients with insufficient upper body strength to keep balance in the early rehabilitation stages; therefore, a mobile robotic walker is indispensable to assist with the overground walking and gait training.

As shown in Figure 1, the human-exoskeleton-walker (HEW) system is presented. Note that in the following sections, the human-exoskeleton system means a subject wearing the exoskeleton robot, and the HEW system means the human-exoskeleton system with the robotic walker.As shown in Figure 1, the human-exoskeleton system is connected to the mobile robotic walker with a solid cantilever; a support joint is attached to the cantilever for the vertical movement assistance and weight supporting during walking. The robotic walker ensures the stability of the human-exoskeleton system in the coronal plane, validly keeping balance and preventing falls.

For patients with gait impairments, movement disorder can severely disrupt the performance of daily activities and increase the risk of falling. Although various existing walkers are owned by seniors, reported statistics show that 33% of people over 60 years fell at least once[1]. We argue that intelligence is essential for a robotic walker to protect the safety of the patients, since primitive assistance devices, such as rollators and walkers, are much more likely to fail[2]. Present-day assistant devices require attentive control of the user while moving[3,4], which could raise safety issues for many patients with insufficient upper body strength and cause bad coordination between the human-exoskeleton system and the robotic walker. A few studies have investigated the task enabling the walker to follow behind the user by detecting his/her trajectory beforehand[5]. However, the gait trajectory of patients with gait impairments is always varying during the rehabilitation stage. As a result, the robotic walker may not be able to follow the patients well. The gait trajectory of the exoskeleton is predefined, so we take the approach of adopting a Coordinated motion planning strategy to generate the appropriate joint angle for the wheels of the robotic walker according to the predefined gait trajectory of the exoskeleton, enabling our walker to follow the movement trend of the user; our walker can then automatically move behind the user, providing mobility support. Furthermore, without an appropriate supporting force offered by the support joint and coordinated movement of the wheels to follow the walking of the human-exoskeleton system, the human-exoskeleton system has to *pull* or *push* the robotic walker forward during walking, which leads to the bad walking posture and unnecessary energy-cost of the human-exoskeleton system. As a result, battery life has always been a severe challenge to the exoskeleton robots. Among commercially available exoskeletons, Indego[6] and Ekso[7]have only 4 h of battery life. Even with the largest battery capacity, ReWalk[8] and SuitX[9] allow for continuous work for not more than 5 h. It is impossible to meet the hospital's demand for all-day rehabilitation training with these exoskeleton robots. Therefore, it is crucial to improve the energy efficiency of the HEW system with an appropriate supporting force offered with the support joint and the coordinated movement of the wheels to follow the natural walking of the human-exoskeleton system.

In the last decades, several approaches have been studied with the body weight supporting (BWS) system for the energy-efficient walking assistance. Sun *et al.* proposed a BWS system for the three-dimensional walking in Cartesian space[10], with the series elastic actuation structure to improve the human-robot interaction performance and reduce the energy cost of the human. Wei *et al.* proposed a surplus force control strategy named active loading compound control for the BWS system, which is used for estimating and improving the loading accuracy[11] and reduces the surplus force and the energy cost. For the mobile robotic walker, Mun *et al.* proposed a mobile robotic walker for the movement of the pelvis of humans, which can be used to facilitate the over-ground walking without altering the normal gait dynamics[12]. Similar structure has been developed in ref[13]. Chugo *et al.* developed a robotic walker to assist with the standing motion and simple walking for the aged person in daily life, which estimates the load of the pelvis, knee and ankle joints of the human body, and generate appropriate joint angle for the support joint of the robotic walker[14]. These mobile robotic

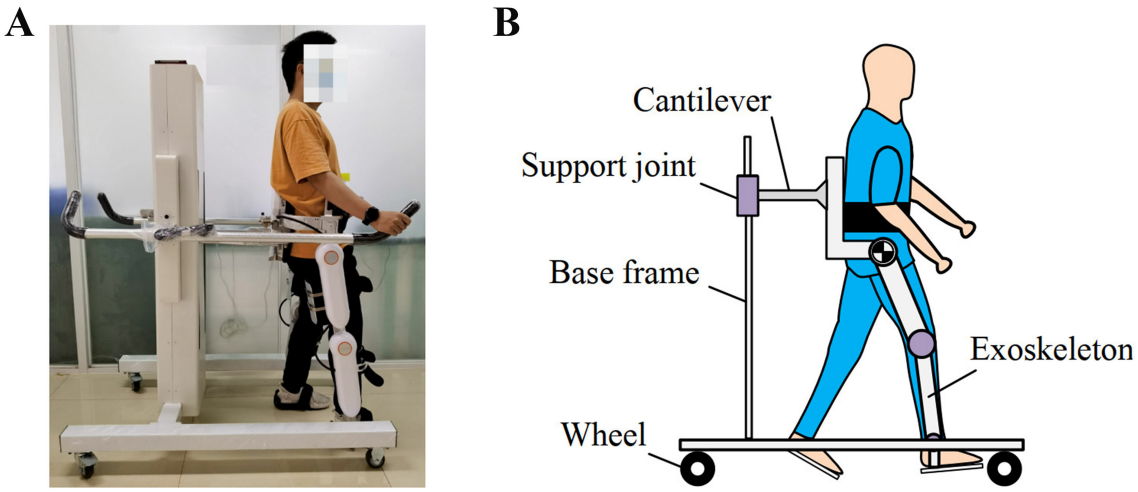

Figure 1. The schematic of the human-exoskeleton-walker system. (A) A real exoskeleton robot with a robotic walker; (B) The support joint and the wheels of the robotic walker shall be controlled to follow the walking of the human-exoskeleton system.

walkers are developed for the energy cost reduction of humans and are not applicable to the HEW system. For optimization-based approaches, Ding *et al.* used Bayesian optimization to identify the peak and offset timing of hip extension assistance that minimizes the energy expenditure of walking with a textile-based wearable device, causing reduced metabolic cost by 17.4% ± 3.2% compared with walking without the device[15]. Song and Collins used human-in-the-loop optimization to largely improve self-selected walking speed through ankle exoskeleton assistance, which achieved a reduced metabolic cost by at most 31%[16]. In addition, Lee and Rosen developed new energy optimization strategies utilizing collision-based ground reaction forces and a discrete Lagrangian to realize the energy recycling of the exoskeleton, achieving a 35% reduction of the normal walking cost of transport[17].

Although the BWS-based approach has demonstrated its energy efficiency, it is mostly used to reduce human's energy cost and is not applicable to the HEW system. In this paper, we focus on the coordinated energy-efficient walking assistance of the HEW system, and the human-in-the-loop optimization for the energy consumption of the human-exoskeleton system is the key research topic. The key points are as follows: First, to find the optimal supporting force of the robotic walker during walking, which can provide the human-exoskeleton system with the body weight support to maximize energy efficiency. Second, to generate appropriate joint angles as the control reference of the wheels to produce a coordinated movement of the robotic walker and the human-exoskeleton system during walking. However, due to the unknown relationship between the energy efficiency and the supporting force, it is difficult to calculate the optimal supporting force during walking. In this paper, a Coordinated Energy-Efficient Control (CEEC) approach is proposed for the HEW system to provide the coordinated movement of the human-exoskeleton system and the robotic walker and maximize the energy efficiency of the HEW system. CEEC consists of a model-free Extremum Seeking Control (ESC) algorithm and a coordinated motion planning approach, which performs real-time seeking of the supporting force and generation of the joint angles of the wheels. The ESC uses a low-frequency perturbation signal to estimate the gradient of the cost function, making it more robust to noisy measurements[18]. The main contributions are summarized as follows:

- The energy efficiency of the HEW system is maximized by the extremum seeking control algorithm in real time to simultaneously tune the supporting force of the support joint. The optimum of the supporting force shifts at different conditions, and our algorithm is suitably fast to track these changes, providing real-time adaptation for different conditions.
- A coordinated motion planning approach is proposed for the HEW system, which performs the coordinated

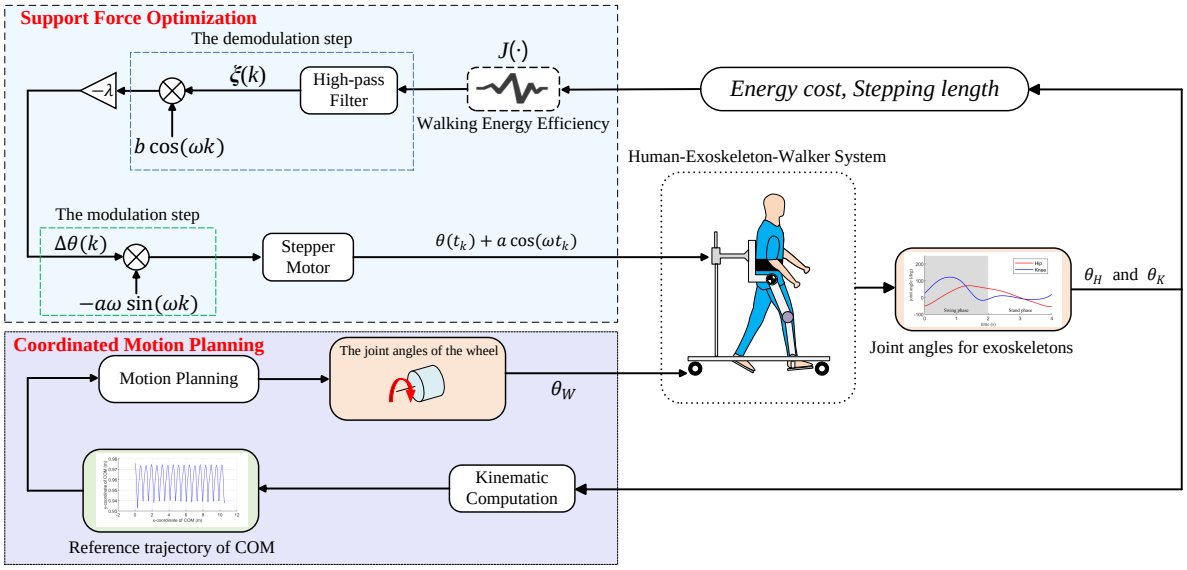

Figure 2. The framework of the proposed approach CEEC. COM: Center of Mass; CEEC: Coordinated Energy-Efficient Control.

assistance of the robotic walker for the human-exoskeleton system during walking. The appropriate joint angle is generated with the predefined gait trajectory of the exoskeleton, enabling our walker to follow the movement trend of the user; our walker can then automatically move behind the user, providing mobility support.

- The efficiency of the proposed approach has been tested on the HEW simulation models; the experimental results indicate that the energy efficiency was improved by 60.16% compared to the conventional robotic walker and the coordination between the human-exoskeleton system and the robotic walker was significantly improved.

The remainder of the manuscript is organized as follows: In Section 2, the detailed design of the proposed CEEC is presented. In Section 3, the simulation experiments of the proposed approach are showcased; the experimental results and discussions are provided in Section 4. In Section 5, we concluded the paper, and some future works are suggested.

2. METHODS

In this section, the design of the CEEC is presented, including the human-in-the-loop optimization of the supporting force and implementation of the coordinated motion planning approach of the wheels. As shown in Figure 2, the framework of the proposed CEEC approach is presented, which consists of two parts: the supporting force optimization and coordinated motion planning. In the following two subsections, these two parts will be introduced in detail.

2.1 The optimization of the supporting force

In this subsection, the real-time optimization of the supporting force is presented, which aims to find the optimal supporting force provided by the support joint of the robotic walker. The structure of the HEW system and the energy cost calculation during walking are outlined in Section 2.1.1, and the implementation of the human-in-the-loop optimization for the supporting force is detailed in Section 2.1.2.

2.1.1 Energy calculation of the HEW system with the supporting force

In this subsection, the energy cost of the human-exoskeleton system is presented, where the energy is determined by the power of the active joints of the exoskeleton. The structure of the HEW system is shown in

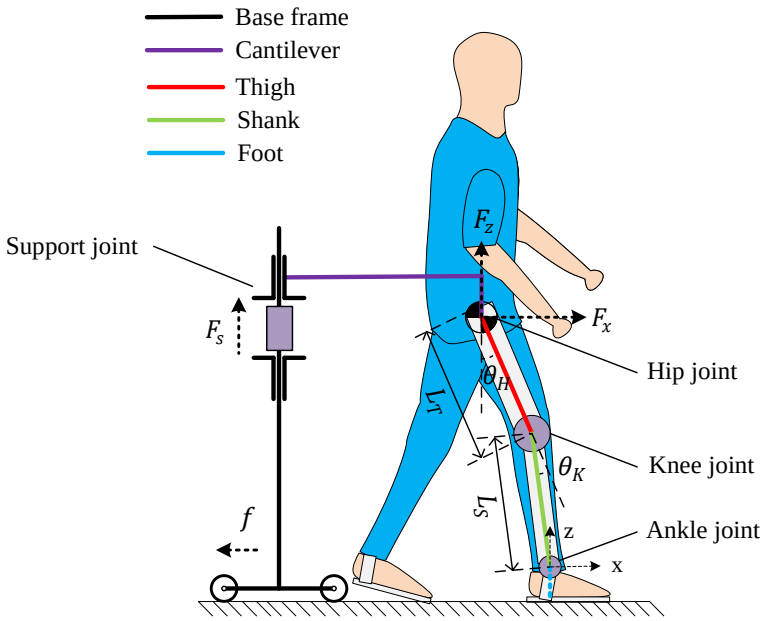

Figure 3. The schematic diagram of HEW system. HEW: Human-exoskeleton-walker.

Figure 3, where the exoskeleton robot includes hip, knee and ankle joints to drive the human-exoskeleton system walking forward. The thighs, calves, and feet of the exoskeleton are interconnected with the corresponding segments of the pilot's lower limbs, ensuring full synchronization between the pilot's lower limb movements and those of the exoskeleton. The supporting force F_S can be supplied by the support joint of the robotic walker, which is used to move the support joint vertically and support the weight of the human-exoskeleton system. The support joint of the robotic walker is actuated with a spring-based mechanism and a stepping motor, which provides a variable supporting force for the human-exoskeleton system with different motor positions. In addition, f represents the horizontal resistance of the robotic walker; F_x and F_z represent the horizontal and vertical components of the supporting force offered by the support leg, respectively. l_T and l_S represent the lengths of the thigh and shank, respectively. θ_H and θ_K represent the hip and knee joint angles of the exoskeleton's support leg, respectively. Note that in this paper, the hip and knee joint angles are sampled from the healthy subjects as the control reference, and the hip and knee joints of the exoskeleton robot are driven by the DC motors with PID position controllers. The ankle of the exoskeleton robot is a passive joint with a spring mechanism, which can be used to avoid the foot drop of the patients.

In this paper, we focus on the movement of the HEW system in the Sagittal plane, and the Center of Mass (COM) of the human-exoskeleton system has a good correspondence in the sagittal plane with the hip joints [19]; therefore, the COM of the human-exoskeleton system is set to the center of two hip joints. The horizontal movement of the COM is solely driven by the exoskeleton support leg, while the vertical movement is influenced by both the support joint and the exoskeleton support leg. Assuming that the ankle joint of the support leg is set as the origin of the Cartesian frame, the COM's position of the human-exoskeleton system can be described when the predefined gait trajectories $\theta_H(t)$ and $\theta_K(t)$ are employed to drive the exoskeleton:

$$\begin{bmatrix} x_{\text{com}}(\theta_H, \theta_K) \\ z_{\text{com}}(\theta_H, \theta_K) \end{bmatrix} = \begin{bmatrix} -\sin(\theta_H) & \sin(\theta_K - \theta_H) \\ \cos(\theta_H) & \cos(\theta_K - \theta_H) \end{bmatrix} \begin{bmatrix} l_T \\ l_S \end{bmatrix}, \tag{1}$$

where the x_{com} and z_{com} represent the horizontal and vertical positions of the COM, respectively. Then, the

horizontal and vertical supporting forces from the support leg F_x and F_z are expressed as follows:

$$\begin{cases} F_x = \ddot{x}_{\text{com}}(m_P + m_W + m_E) + f, \\ F_z = (\ddot{z}_{\text{com}} + g)(m_P + m_E) - F_s, \end{cases} \tag{2}$$

where m_P, m_W and m_E represent the masses of the human subject, the robotic walker, and the exoskeleton robot, respectively. $\ddot{x}_{\text{com}}$ and $\ddot{z}_{\text{com}}$ are the second derivatives of the COM's position x_{com} and z_{com}. g is the constant gravitational acceleration. The torques of the hip and knee joints of the exoskeleton support leg can be calculated as follows:

$$\begin{bmatrix} \tau_H \\ \tau_K \end{bmatrix} = \begin{bmatrix} l_T & l_S \\ 0 & l_S \end{bmatrix} \begin{bmatrix} \cos(\theta_H) & \sin(\theta_H) \\ \cos(\theta_H - \theta_K) & \sin(\theta_H - \theta_K) \end{bmatrix} \begin{bmatrix} F_x \\ F_z \end{bmatrix}, \tag{3}$$

where τ_H and τ_K are the torques of the hip and knee joints. As a result, the power of the exoskeleton robot is determined by the joint torques τ_H and τ_K and the angular velocity of the joint $\dot{\theta}_H$ and $\dot{\theta}_K$. Let us take the hip joint as an example; the power of the hip joint's motor P_m is calculated as:

$$\begin{cases} P_m = I^2 \cdot R_m + \tau_m \cdot \dot{\theta}_m, \\ \tau_m = \tau_H / r = K_m \cdot I, \\ \dot{\theta}_m = \dot{\theta}_H / r, \end{cases} \tag{4}$$

where τ_m and $\dot{\theta}_m$ represent the torque and angular velocity of the motor in the hip joint, respectively. I represents the current of the motor, and r is the reduction ratio. Besides, R_m and K_m represent the resistance and torque constant of the motor, respectively. The first item of P_m in Equation (4) represents the thermal power, while the second item indicates the mechanical power. With the power of the motors in the joints of the support leg, the energy consumption of the exoskeleton support leg during the stance phase can be calculated as follows:

$$E = \int_0^T (P_m^H + P_m^K) dt, \tag{5}$$

where P_m^H and P_m^K denote motor power of the hip and knee joints, respectively. T signifies the duration of the stance phase in one gait cycle.

Based on the Equations (2)-(4), we can find that the torques of the hip and knee joints are decreased as the supporting force F_s increases, i.e., the energy cost of the exoskeleton robot is decreased with increasing F_s. However, if the supporting force is too large, the human-exoskeleton system will be lifted off the ground, and the friction between the ground and the exoskeleton's foot will be reduced, resulting in an abnormal walking posture of the human-exoskeleton system and even with slipping over the ground. Therefore, finding the appropriate supporting force to minimize the energy consumption and prevent slipping is critical. Now, let us construct an objective function to denote the energy efficiency:

$$J(\cdot) = E / S, \tag{6}$$

where E denotes the energy consumption of both hip and knee joints of the support leg during the stance phase in one gait cycle; S represents the stepping length for one step. Consider the value of the objective function as Total Cost of Transport (TCoT). Now, let us find a way to solve the objective function and find the optimal supporting force.

2.1.2 Real-time optimization of the supporting force

In this subsection, the real-time optimization of the supporting force, which employs the discrete-time ESC approach, is presented. ESC is a model-free adaptive control method that finds an optimum set-point in order to minimize/maximize an objective function, whose analytical expression might be unknown [20–23]. Kumar *et al.* proposed a modified structure of the discrete-time ESC by introducing a stepper motor with an integrator [24,25]. In this modified structure, the ESC integration is performed by the motor dynamics itself. Moreover,

the stepper motor has the same characteristics as the zero-order holder; it does not have any closed-loop encoder feedback for position control. Instead, it accepts a variation in the motor location as an input command rather than the final motor location. In this paper, we used the variation in the motor location to tune the supporting force of the support joint.

The block diagram of the modified ESC used in this paper is shown in Figure 4, where the workflow of the ESC is as follows. Firstly, a periodic disturbance signal of small amplitude $d_1(k) = -a\omega \sin(\omega t_k)$ called the dither signal is added to the commanded change in the motor location $\Delta\theta(k)$ in the modulation step.

Assuming that the stepper motor dynamics is modeled as a cascade connection of a zero-order holder and a continuous-time integrator. The zero-order holder holds the sample $\Delta\theta(k) + d_1(k)$ constant for one sampling interval ΔT. Denoting that t_k is the sampling time, the expression for $\dot{\theta}(t_k) \approx \Delta\theta(k)/\Delta T - a\omega \sin(\omega t_k)$; then, the integrator dynamics of the stepper motor outputs $\theta(t_k) + a\cos(\omega t_k)$, where $\theta(t_k)$ is the stepper motor's location at t_k. The output of the stepper motor is used to tune the supporting force by changing the position of the stepper motor in the support joint. Then, the torques of the hip and knee joints are sampled in one gait cycle, and the power of the hip and knee joints is calculated according to the Equation (4). Next, the power is multiplied by the sampling interval ΔT, and we summed them up to get the total energy consumption of the hip and knee joints as E. Therefore, the objective function can be rewritten as:

$$J(\cdot) = E/S = J((\theta(k) + a\cos(\omega k))), \tag{7}$$

and the Taylor series approximation of $J(\cdot)$ is expressed as follows:

$$\begin{aligned} J(\cdot) &\approx J(\theta(k)) + J'(\theta(k))a\cos(\omega k) + \frac{J''(\theta(k))}{2}a^2\cos^2(\omega k) \\ &= J(\theta(k)) + J'(\theta(k))a\cos(wk) + \frac{a^2J''(\theta(k))}{4}(1 + \cos 2(\omega k)), \end{aligned} \tag{8}$$

where J' and J'' are the first and the second derivatives of $J(\cdot)$ with respect to θ. Then, the objective function measurements in Equation (8) are passed through a high-pass filter HPF to remove the DC components $J(\theta(k))$ and $a^2J''(\theta(k))/4$ to give

$$\xi(k) = J'(\theta(k))a\cos(\omega k) + \frac{a^2J''(\theta(k))}{4}\cos(2\omega k). \tag{9}$$

In the demodulation step, $\xi(k)$ is multiplied by another dither signal $b\cos(\omega k)$ and scaled by a gain $-\lambda$ to generate

$$\begin{aligned} \Delta\theta(k) &= -\lambda[J'(\cdot)a\cos(\omega k) + \frac{a^2J''(\cdot)}{4}\cos(2\omega k)]b\cos(\omega k)] \\ &= -\lambda[\frac{abJ'(\cdot)}{2}[1 + \cos(2\omega k)] + \frac{a^2bJ''(\cdot)}{4}\cos(2\omega k)\cos(\omega k)], \end{aligned} \tag{10}$$

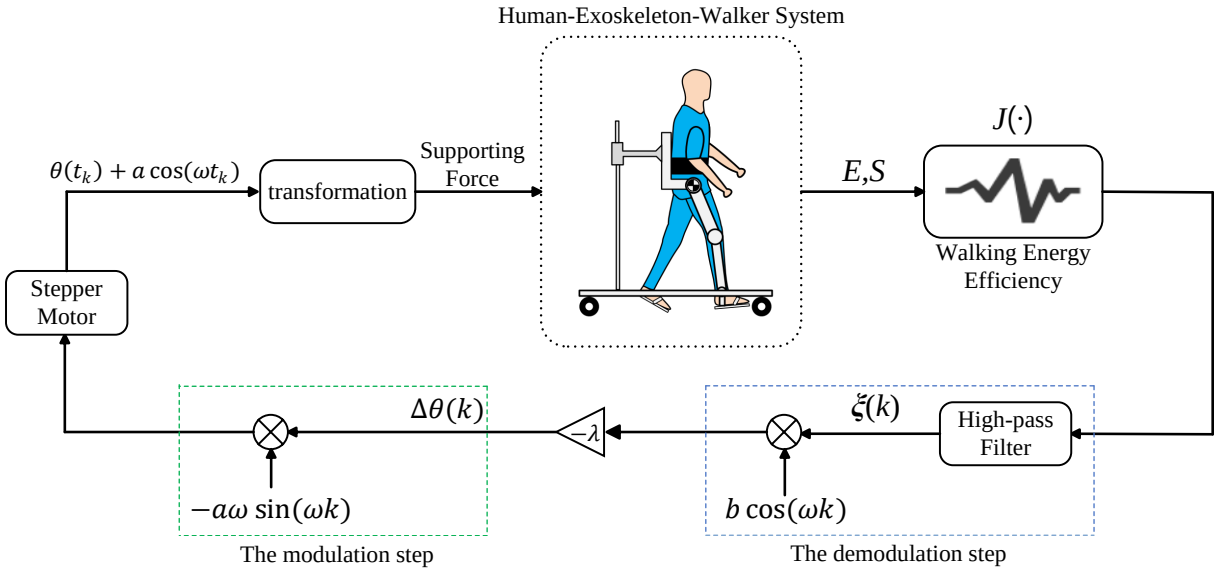

Figure 4. The block diagram of ESC. ESC: Extremum Seeking Control.

where $\Delta\theta(k)$ indicates the amount that the stepper motor should be moved to minimize the TCoT, which realizes the supporting force adaptive tuning. From Equation (10), it can be seen that $\Delta\theta(k)$ consists of a DC component, which is proportional to $J'(\cdot)$, and contains other higher frequency terms.

Following standard manipulations [26], the equations of ESC can be updated as follows:

$$\xi(k) = -h\xi(k-1) + J(\theta(k)) - J(\theta(k-1)), \tag{11}$$

$$\Delta\theta(k) = -\lambda[\xi(k)b\cos(\omega k)], \tag{12}$$

where λ is the adaptation gain, and $h \in (0, 1)$ is the HPF cut-off frequency.

Overall, with the proposed real-time optimization approach, the optimal supporting force can be found in real time by walking several steps overground with the HEW system. As a result, the energy cost of the HEW system will be reduced to the minimum value without slipping overground.

2.2 The coordinated motion planning of the robotic walker

The coordinated motion planning is to make the human-exoskeleton system and the robotic walker move coordinately and avoid the "pull" or "push" between them. As shown in Figure 2, the coordinated motion planning is based on the hip and knee joint angles of the exoskeleton robot. As shown in Figures 5 and 6, there are four wheels of the robotic walker, and all wheels rotate around the Y axis.

As we mentioned in Figure 1, the exoskeleton robot is connected to the robotic walker with a solid cantilever; therefore, the horizontal movement of the robotic walker is the same as the COM of the human-exoskeleton system. Note that if the wheels are passive without any power, there is no active movement of the robotic walker, and the human-exoskeleton system has to pull or push the robotic walker while walking overground. If the wheels are actuated with the DC motors, they can drive the robotic walker to follow the movement of the human-exoskeleton system and avoid the movement conflict between the human-exoskeleton system

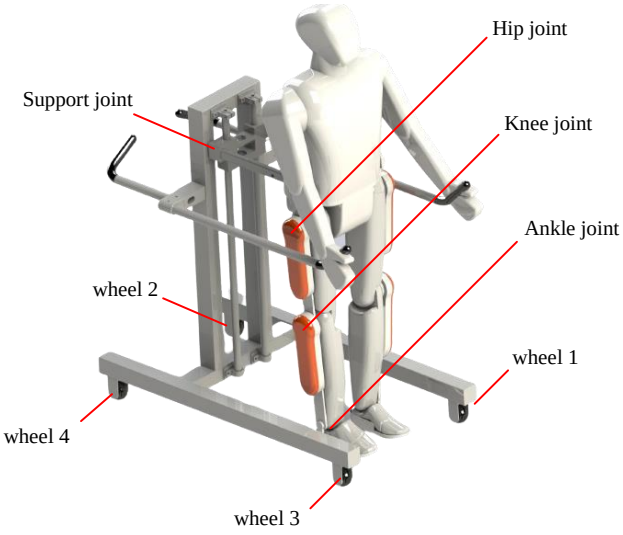

Figure 5. The simulation model of the HEW system. HEW: Human-exoskeleton-walker.

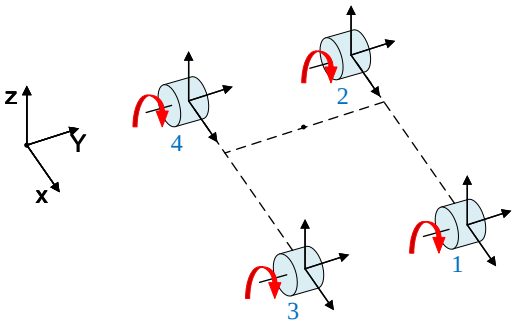

Figure 6. The wheels of the robotic walker.

and the robotic walker. Therefore, the question is how to control these wheels to drive the robotic walker to coordinately follow the movement of the human-exoskeleton system.

Based on Equation (1), the movement of the COM during walking can be calculated with the joint angles of the exoskeleton robot. Additionally, the horizontal movement of COM can be discretized with a constant unit time Δt, taking i as an index for discretization, then

$$t_i = \Delta t \cdot i, \quad i = 0, 1, 2, \ldots \tag{13}$$

where Δt can be set to some small positive value such as $\Delta t = 0.005$ s. The COM horizontal displacement from t_{i-1} to t_i can be calculated as follows:

$$\Delta x_i = x_i - x_{i-1}, \quad i = 1, 2, \ldots \tag{14}$$

where x_i represents the horizontal position of the COM at t_i. Based on the COM horizontal displacement Δx_i, the increment of the joint angles for the wheels from t_{i-1} to t_i is calculated as follows:

$$\Delta\theta_i = \Delta x_i / R_w, \tag{15}$$

where R_w is the radius of the wheels on the robotic walker. Now, with the horizontal movement of the human-exoskeleton system, the reference joint angles of the wheels can be obtained, and the human-exoskeleton system and the robotic walker can be moved coordinately.

3. EXPERIMENTS

In this section, simulation experiments are conducted with the constructed HEW simulation models in the robot simulation platform CoppeliaSim (https://www.coppeliarobotics.com). The simulation model is shown in Figure 5; the model retains the same configuration of degrees of freedom illustrated in Figure 3, where the wheels are controlled with the PID position controllers and the support joint is controlled in the torque mode to support the weight of the human-exoskeleton system. The torques and the trajectories of the COM's movement can be obtained, and the power and the energy cost of the HEW system can be calculated, with the proposed CEEC approach; the optimal supporting force can be found after several walking steps. In addition to this, the tracking performance of the COM's movement can be used to evaluate the coordination between the human-exoskeleton system and the robotic walker.

3.1. Experimental setup

To evaluate the performance of the proposed CEEC approach, several experiments were designed in the simulation experiments. Firstly, the hip and knee joint angles used in the experiment are sampled from the healthy subject, as shown in Figure 7, where the joint angles in swing and stance phases are for the swing leg and the support leg, respectively. The mass distribution of the human-exoskeleton system (torso, thigh, shank, and foot) follows average human anthropometry[27], as shown in Table 1, and the length of the thigh and shank is set to 0.45 m, which is similar to the subject with the body height of 1.75 m.

Overall, the total mass of the human subject, the exoskeleton, the robotic walker, and other parameters for the simulation experiments are shown in Table 2. Note that the parameters for the motors in hip and knee joints refer to the manual of the DC motors used in our exoskeleton robots shown in Figure 1.

To evaluate the proposed CEEC approach and compare it with others, four experiments were designed, each assigned a distinct name.

- The first one is the "baseline"; there was no active assistance of the robotic walker, i.e., the human-exoskeleton system had to pull the robotic walker forward during walking.
- The second one is the Coordinated Motion Planning ("CMP"); there was only the active assistance from the wheels with the generated coordinated motion planning, i.e., the wheels were controlled with the reference joint angles generated in Section 2.2. In addition, there was no supporting force from the support joint.
- The third one is the "ESC"; there was only the supporting force from the support joint under the ESC strategy, with no active assistance from the wheels.
- The last one is the "CEEC"; there was active assistance from both the support joint and wheels; the supporting force was optimized with the ESC strategy; the wheels were controlled with the reference joint angles in Section 2.2.

To evaluate the adaption of the proposed CEEC approach for different subjects, three subject simulation models with various masses are employed in the experiment [Table 3]. Note that the ESC strategy is an online iterative algorithm, and the initial value of the supporting force should be set at the beginning of the experiment. Therefore, two distinct initial supporting forces were given [Table 3].

For each trial of the experiment, seventeen steps (the first step and eight gait cycles) were conducted to test the efficiency of the proposed approach. Note that the first is a special step from the standing upright posture to walking; therefore, the control strategy only works in the last sixteen steps. The sampling rate is 20 Hz, and the gait cycle is two seconds with two steps. The TCoT was computed with the sampled torque of the support leg's hip and knee joints after each gait cycle. The parameters of ESC were selected as follows: a = 1.6, b = 0.8, ω = 0.8 Hz, h = 0.4 Hz, λ = -6.

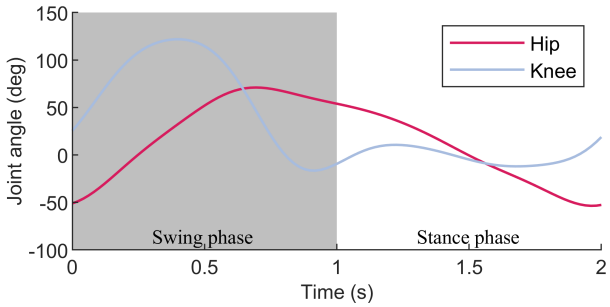

Figure 7. The joint angles of the exoskeleton's hip and knee joints.

Table 1. Parameters for human and exoskeleton simulation models

Segment part	Mass (kg)		Length (m)
	Human	Exoskeleton	Human-exoskeleton
Upper body	42	5	
Thigh	5.7	4	0.45
Shank	2.5	4	0.45
Foot	0.8	0.5	0.28
Total	60	22	

Table 2. Other parameters for simulation and energy cost computation

Parameters	Description	Value
m_W	Base frame mass	40 kg
m_P	Human subject	60 kg
m_E	Exoskeleton mass	22 kg
μ	Coefficient of friction	0.71
f	Resistance of the walker	10 N
g	Gravitational acceleration	10 m/s^2
r	Reduction ratio of exoskeleton reducers	60
K_m	Torque constant of exoskeleton motors	0.162 Nm/A
R_m	Motor resistance of exoskeleton motors	0.23 Ω
R_w	The radius of the wheels	0.038 m

Table 3. Different scenarios for validating the CEEC

Index	Mass of the subject (kg)	Initial supporting force (N)
A1	40	300
A2	60	300
A3	80	300
B1	40	400
B2	60	400
B3	80	400

CEEC: Coordinated Energy-Efficient Control.

3.2 Simulation experiments recording

The snapshots of the four experiments (baseline, CMP, ESC, CEEC) are shown in Figure 8, where each row corresponds to one of the four different experiments, i.e., baseline, CMP, ESC and CEEC, respectively. It is significant that with diverse control strategies, the COM's tracking performances vary.

The snapshots of the experiments with three different subjects and the CEEC control approach are shown in Figure 9. Since the CEEC is adaptive to various scenarios, the walking performance is similar for subjects with varying masses.

For a more detailed presentation of the whole walking experiment, please refer to the Supplementary Video.

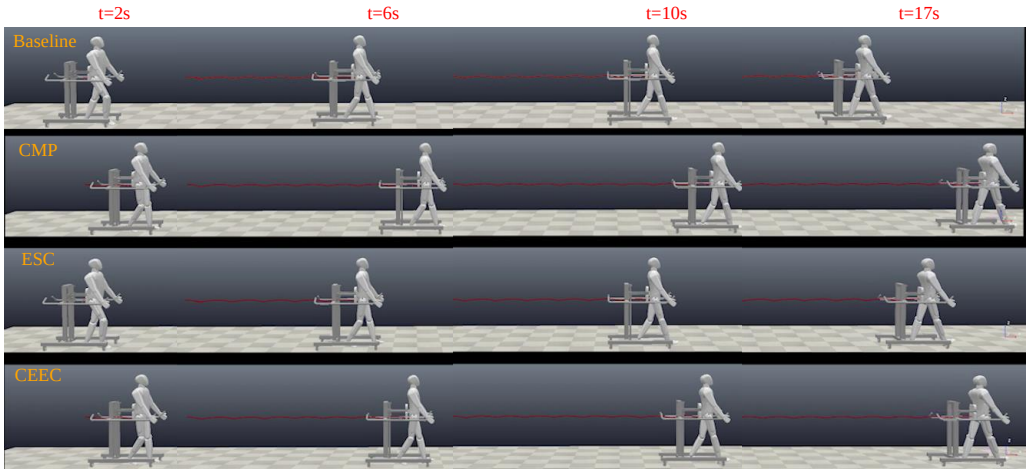

Figure 8. The comparison of walking experiments with different control strategies. CMP: Coordinated Motion Planning; ESC: Extremum Seeking Control; CEEC: Coordinated Energy-Efficient Control.

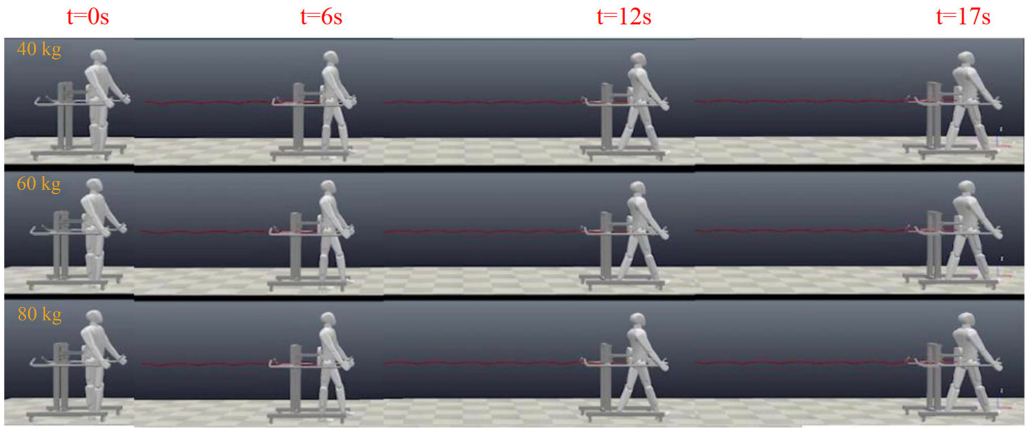

Figure 9. The comparison of walking experiments for different subjects.

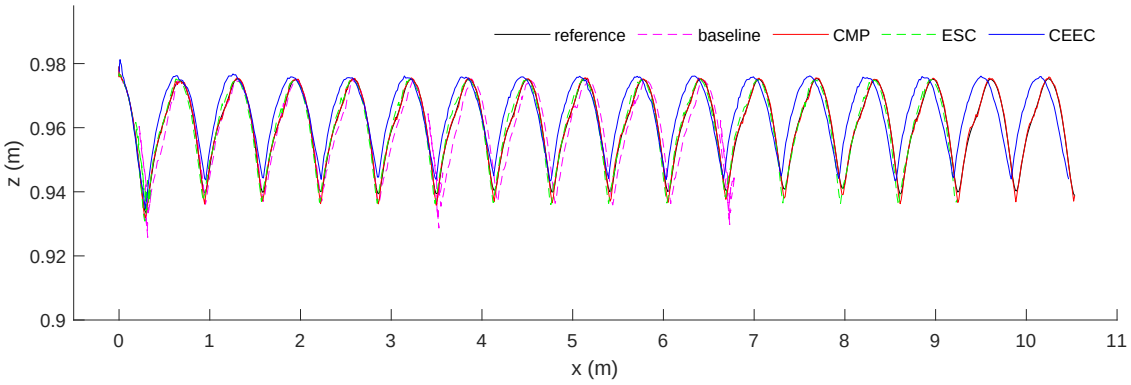

Figure 10. The comparison of COM trajectories tracking performance with different control strategies. (1) Reference: the reference COM trajectories; (2) Baseline: the human-exoskeleton walks without any assistance of the robotic walker; (3) CMP: the HEW system walks with only the active wheel movements; (4) ESC: the HEW system walks with only the supporting force under the ESC strategy; (5) CEEC: the HEW system walks with the proposed coordinated energy-efficient control approach. CMP: Coordinated Motion Planning; ESC: Extremum Seeking Control; CEEC: Coordinated Energy-Efficient Control; COM: Center of Mass; HEW: human-exoskeleton-walker.

4. RESULTS AND DISCUSSION

4.1 Experimental results for the comparison with the COM's trajectory tracking and the energy cost

First of all, the comparison of COM's trajectories tracking performance with baseline, CMP, ESC and CEEC during the whole walking experiments are shown in Figure 10. Note that the HEW system is moving in the Sagittal plane; therefore, only the x and z positions of the COM are presented. The black solid curve is the reference trajectory of the COM calculated from the reference joint angles based on the Equation (1), the dashed purple curve is the COM's trajectory with the baseline (with no supporting force and no assistance from wheels), the solid red curve is the COM's trajectory with the CMP (with only active assistance from wheels and no supporting force), the dashed green curve is the COM's trajectory with the ESC (with only supporting force and no assistance from wheels), and the solid blue curve is the COM's trajectory with the CEEC (with both supporting force and assistance from wheels).

To compare the trajectory tracking of four cases, the mean squared error (MSE) of four cases relative to the reference COM trajectories was calculated as:

$$MSE = \frac{1}{n}\sum_{i=1}^{n}[(X_i - \hat{X}_i)^2 + (Z_i - \hat{Z}_i)^2] \tag{16}$$

The calculated MSE of four cases was shown in Table 4.

From the trajectory tracking comparison, we can find that in the baseline case, due to no active assistance from the robotic walker, the human-exoskeleton system has to pull the robotic walker forward during walking, the COM's trajectory tracking is bad, and the final position of the COM is far away from the desired position. In the CMP case, since there is active assistance of the wheels with the coordinated motion generated with the reference COM trajectory, the tracking performance of the COM is good. For the ESC and CEEC cases, since a supporting force exists, the COM's trajectory tracking is better than the baseline, and especially for the CEEC case, the COM's trajectory tracking is better than the ESC case. Note that in the first several steps, the supporting force is not optimal, and the ESC algorithm is tuning to find the optimal supporting force, which results in a bad performance. However, after several steps of optimization, the optimal supporting force is found, and the COM's trajectory tracking is better. This is the reason why the MSE of CEEC is a little bigger than the MSE of CMP.

Above all, for the COM's trajectory tracking, CEEC is better than the ESC and baseline but worse than the CMP. Now, let us see the energy cost during walking with these different strategies [Figure 11]. From the bars presented in Figure 11, we can see that in the baseline case, the energy cost is much higher than in any other method. In the CMP case, the energy cost is always similar during the walking. In ESC and CEEC cases, the energy cost is very high at the beginning of the walking and decreases after several steps; this is because, at the first several steps, the ESC algorithm needs to iteratively update the supporting force and find the optimal one, which leads to a bad walking performance and high energy cost. After several steps, the energy cost is reduced, and the CEEC is better than the ESC; this is because the CEEC not only optimizes the supporting force but also provides horizontal coordinated walking assistance by wheels.

Overall, considering the COM's trajectory tracking performance and the energy cost, the CEEC is the best approach for the HEW system to finish coordinated energy-efficient overground walking.

Table 4. The MSE of four cases

Cases	Description	MSE
Baseline	With no supporting force and no assistance from wheels	4.0841
CMP	With only active assistance from wheels and no supporting force	0.0019
ESC	With only supporting force and no assistance from wheels	1.4496
CEEC	With both supporting force and assistance from wheels	0.0027

MSE: Mean squared error; CMP: Coordinated Motion Planning; ESC: Extremum Seeking Control; CEEC: Coordinated Energy-Efficient Control.

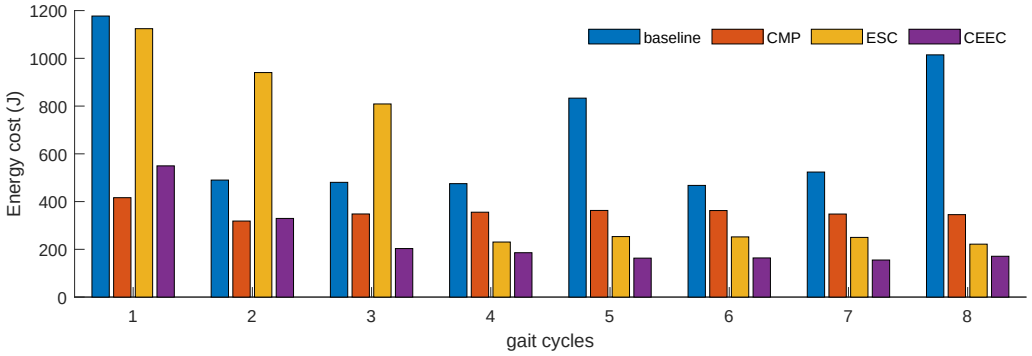

Figure 11. The comparison of energy cost with different control strategies. CMP: Coordinated Motion Planning; ESC: Extremum Seeking Control; CEEC: Coordinated Energy-Efficient Control.

4.2 Experimental results for the comparison of subjects with different masses

To validate the adaptive capacity of the CEEC algorithm in various scenarios, subjects with varying masses are employed and different initial support forces for CEEC are given [Table 3]. As mentioned before, there are eight gait cycles of each experiment; the hip and knee joint torques of the support leg were recorded with the sampling frequency of 20 Hz for the CEEC algorithm.

The variation of the supporting force for different subjects and initial supporting force settings are shown in Figure 12, and all support forces will be iteratively updated and converged to the optimal one after several steps of walking. Note that for distinct subjects, the final optimal support forces vary and mainly depend on the masses of the subject; this is because a bigger supporting force is needed for a heavier subject. So for the heaviest subject (A3 and B3) with the mass of 80 kg, the required supporting force is much bigger than the lightest subject (A1 and B1) with the mass of 40 kg.

The variation of the TCoT for different subjects and initial supporting force settings are shown in Figure 13. The TCoT can be calculated with the Equations (4)-(6), where the joint torques for during the walking can be found in Figure 14. Then, the support leg's energy consumption in one gait cycle can be obtained by integrating the power of hip and knee joints over the gait cycle; the stepping length is also obtained. Similar to the variation of the supporting force, the TCoT for diverse subjects could converge to an almost constant value after three gait cycles. Note that for the same subject, the TCoT converged to a closed value after several steps; this is because the CEEC is an iterative updated algorithm and will tune the supporting force online; even with different initial supporting force settings, the final optimal supporting force only depends on the subject's masses in these experiments.

The final converged supporting force and the improvement of the energy efficiency are shown in Table 5, where the TCoT in the baseline case was chosen to be compared with the CEEC case. To confirm that these values are optimal, the three control groups in Table 5 were selected to be compared with the optimal supporting force.

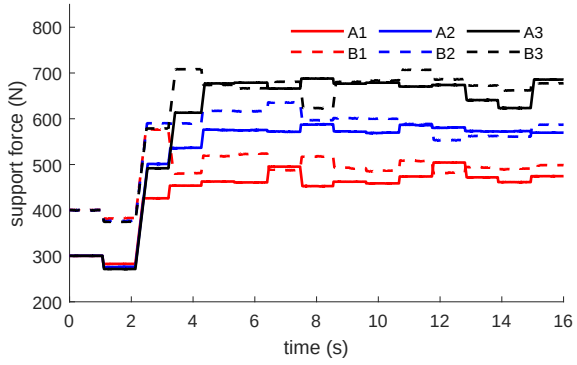

Figure 12. The variation of the supporting force during walking.

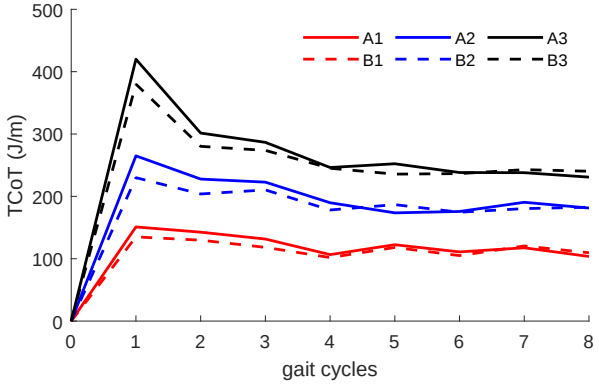

Figure 13. The value of the TCoT during walking. TCoT: Total cost of transport.

Table 5. The optimal supporting force and the improvement of the energy efficiency with the CEEC

Index	Converged supporting force (N)	Converged TCoT (J/m)	TCoT of baseline (J/m)	TCoT reduction
A1 & B1	487	130	309.4	58%
A2 & B2	579	181	454.7	60.90%
A3 & B3	682	245	638.7	61.60%

CEEC: Coordinated Energy-Efficient Control.

In the experiments, the different supporting forces were set for the support joint, whose values are selected in the interval with the converged supporting force as the midpoint. The selected values of constant supporting force and the comparison of the TCoT with the converged one are shown in Table 6. From Table 6, when the converged supporting force was increased or decreased, the TCoT always increased. Looking at Equations (2)-(4), it is intuitive that the elevation of the supporting force leads to the reduction of the energy cost. However, if the supporting force is bigger than the optimal one, it may cause severe slippage in the human-exoskeleton system. Despite the reduced energy cost, the TCoT also rises. When the supporting force is smaller than the optimal one, the energy cost increases without slippage, similarly causing the TCoT to increase. As a result, the converged supporting forces of the three control groups are optimal.

The optimal supporting force in the table is the average final converged value in Figure 12, and the optimal TCoT is the average final converged value in Figure 13. Compared with the baseline, the CEEC reduced the TCoT by 58%, 60.9% and 61.6%, respectively. In other words, the average improvement of the energy efficiency can be calculated with these three values, i.e., 60.16%.

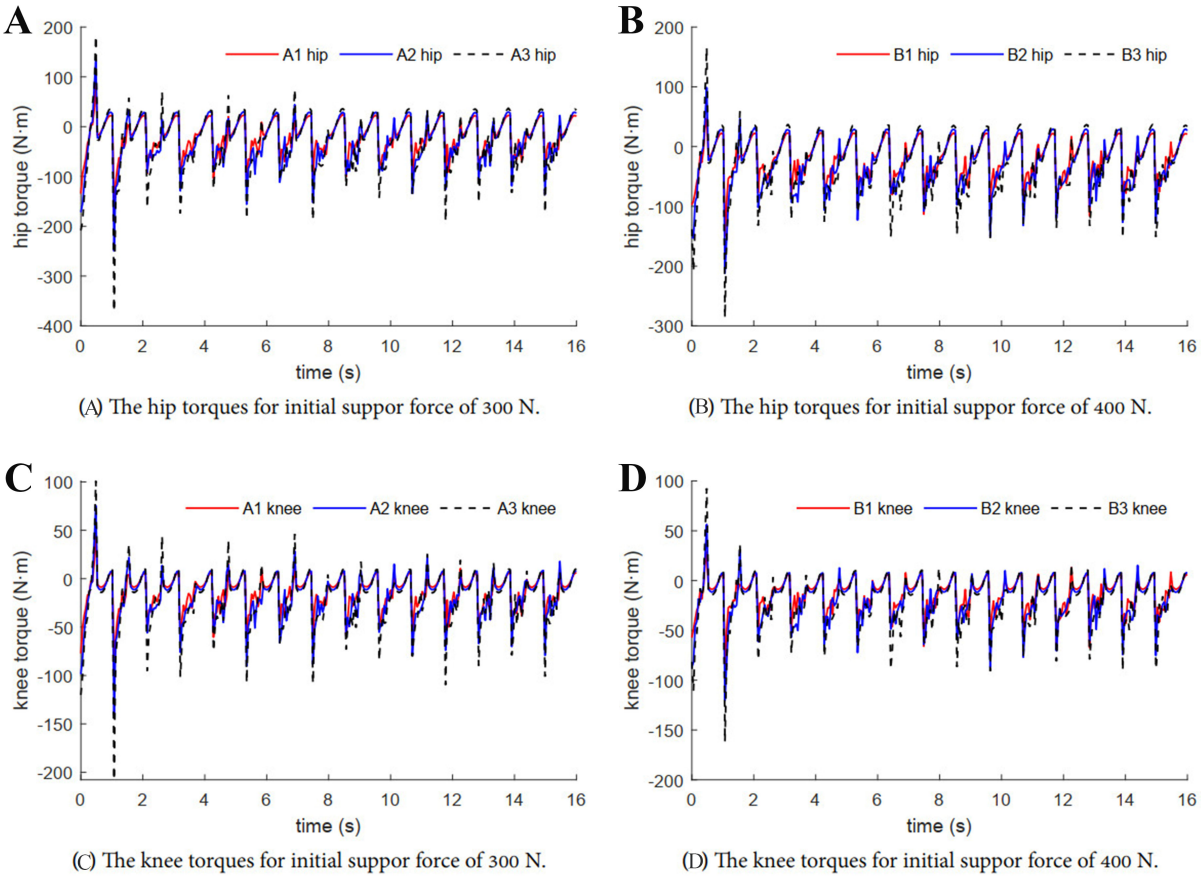

Figure 14. The variation of the hip and knee joint torques during walking for different subjects.

Table 6. The comparison of the TCoT with different supporting forces

Index	Supporting force (N)	TCoT(J/m)	TCoT elevation
A1 & B1	687	161	23.80%
	587	148	13.80%
	487	130	Baseline
	387	165	26.90%
	287	250	92.30%
A2 & B2	779	210	16%
	679	196	8.29%
	579	181	Baseline
	479	231	27.62%
	379	263	45.30%
A3 & B3	882	290	18.37%
	782	263	7.35%
	682	245	Baseline
	582	309	26.12%
	482	353	44.08%

TCoT: Total cost of transport.

The variations of the hip and knee joint torques in the experiments are shown in Figure 14. With the iterative update of CEEC, the peak joint torques of both hip and knee joints in all scenarios are reduced significantly after several steps of walking with increasing supporting force, which means the CEEC is an online real-time optimization approach for the HEW system. Note that for different subjects and initial settings of the supporting force, the joint torques can be online optimized, and for subjects with varying masses, the required joint

torques are distinct. For example, in Figure 14, the red solid curve with a lighter subject mass is smaller than the black dashed curve with a heavier subject mass.

Overall, the experimental results indicate the CEEC approach proposed in this paper can realize the coordinated energy-efficient walking assistance for the HEW system, resulting in a significant improvement. However, If you are only concerned with the COM tracking effect, CMP is the better approach. Methods can be chosen according to the actual situation.

5. CONCLUSIONS AND FUTURE WORK

In this paper, a CEEC approach is proposed for the HEW system, which is based on the discrete-time extremum seeking control and the coordinated motion planning strategies. The proposed approach could automatically tune the supporting force in real time, and adaptive to different subjects, and drive the robotic walker to follow the movement of the COM. Optimal supporting force and coordinated joint angles can be generated with the proposed approach for the robotic walker to assist the human-exoskeleton systems in implementing high energy-efficient walking. In the future, the efficiency of the method should be tested in more different scenarios, such as with varied gait patterns, and applied to the real HEW systems.

DECLARATIONS

Authors' contributions

Conception and design of the study and performed data analysis: Yang C, Zou C, Peng Z
Manuscript writing: Yang C, Zou C
Materials support and experiments set up: Zhang X, Cheng H
Performed data acquisition and analysis of the study: Zhang X, Zhang L
Manuscript review and correction: Huang R, Cheng H

Availability of data and materials

Not applicable.

Financial support and sponsorship

This work was supported by the National Key Research and Development Program of China under Grant 2018AAA0102504, the National Natural Science Foundation of China (No. 62203089, No. 62003073, No. 62103084, No. 62303092), the Project funded by China Postdoctoral Science Foundation under Grant 2021M700695, the Sichuan Science and Technology Program (2022NSFSC0890, 2021YFS0383, 2023YFG0024, 2022YFS0570, 2022NSFSC0865), and the Fundamental Research Funds for the Central Universities (ZYGX2022YGRH003, ZYGX2021YGLH003).

Conflicts of interest

All authors declared that there are no conflicts of interest.

Ethical approval and consent to participate

Not applicable.

Consent for publication

Not applicable.

REFERENCES

1. Luz C, Bush T, Shen X. Do canes or walkers make any difference? Nonuse and fall injuries. *Gerontologist* 2015;57:211-8. DOI
2. Bertrand K, Raymond MH, Miller WC, Martin Ginis KA, Demers L. Walking aids for enabling activity and participation: a systematic review. *Am J Phys Med Rehabil* 2017;96:894-903. DOI
3. Di P, Hasegawa Y, Nakagawa S, et al. Fall detection and prevention control using walking-aid cane robot. *IEEE/ASME Trans Mechatron* 2016;21:625-37. DOI
4. Xu W, Huang J, Cheng L. A novel coordinated motion fusion-based walking-aid robot system. *Sensors* 2018;18:2761 DOI
5. Moustris GP, Tzafestas CS. Intention-based front-following control for an intelligent robotic rollator in indoor environments. In: 2016 IEEE Symposium Series on Computational Intelligence (SSCI); 2016 Dec 6-9; Athens, Greece. IEEE; 2016. pp. 1-7. DOI
6. Tefertiller C, Hays K, Jones J, et al. Initial outcomes from a multicenter study utilizing the indego powered exoskeleton in spinal cord injury. *Top Spinal Cord Inj Rehabil* 2018;24:78-85. DOI
7. Read E, Woolsey C, McGibbon CA, O'Connell C. Physiotherapists' experiences using the Ekso bionic exoskeleton with patients in a neurological rehabilitation hospital: a qualitative study. *Rehabil Res Pract* 2020;2020:2939573. DOI
8. Esquenazi A, Talaty M, Packel A, Saulino M. The ReWalk powered exoskeleton to restore ambulatory function to individuals with thoracic-level motor-complete spinal cord injury. *Am J Phys Med Rehabil* 2012;91:911-21. DOI
9. Koljonen PA, Virk AS, Jeong Y, et al. Outcomes of a multicenter safety and efficacy study of the SuitX phoenix powered exoskeleton for ambulation by patients with spinal cord injury. *Front Neurol* 2021;12:689751. DOI
10. Sun Y, Lei Y, Zou W, Li J, Yu N. Real-time force control of an SEA-based body weight support unit with the 2-DOF control structure. In: 2018 IEEE International Conference on Real-time Computing and Robotics (RCAR); 2018 Aug 1-5; Kandima, Maldives. IEEE; 2018. pp. 390-94. DOI
11. Wei C, Qin T, Meng X, Qiu J, Wang Y, Li B. Surplus force control strategy of an active body-weight support training system. In: Liu XJ, Nie Z, Yu J, Xie F, Song R, editors. Intelligent Robotics and Applications. ICIRA 2021. Lecture Notes in Computer Science, vol 13014. Cham: Springer; 2021. pp. 153-62. DOI
12. Mun KR, Guo Z, Yu H. Development and evaluation of a novel overground robotic walker for pelvic motion support. In: 2015 IEEE International Conference on Rehabilitation Robotics (ICORR); 2015 Aug 11-14; Singapore. IEEE; 2015. pp. 95-100. DOI
13. Song Z, Chen W, Wang W, Zhang G. Dynamic modeling and simulation of a body weight support system. *J Healthc Eng* 2020;2020:2802574. DOI
14. Chugo D, Morita Y, Yokota S, Sakaida Y, Takase K. A robotic walker for standing assistance with realtime estimation of a patient's load. In: 2012 12th IEEE international workshop on advanced motion control (AMC); 2012 Mar 25-27; Sarajevo, Bosnia and Herzegovina. IEEE; 2012. pp. 1-6. DOI
15. Ding Y, Kim M, Kuindersma S, Walsh CJ. Human-in-the-loop optimization of hip assistance with a soft exosuit during walking. *Sci Robot* 2018;3:eaar5438. DOI
16. Song S, Collins SH. Optimizing exoskeleton assistance for faster self-selected walking. *IEEE Trans Neural Syst Rehabil Eng* 2021;29:786-95. DOI
17. Lee H, Rosen J. Lower limb exoskeleton - energy optimization of bipedal walking with energy recycling - modeling and simulation. *IEEE Robot Autom Lett* 2023;8:1579-86. DOI
18. Stanković MS, Stipanović DM. Extremum seeking under stochastic noise and applications to mobile sensors. *Automatica* 2010;46:1243-51. DOI
19. Xi R, Zhu Z, Du F, Yang M, Wang X, Wu Q. Design concept of the quasi-passive energy-efficient power-assisted lower-limb exoskeleton based on the theory of passive dynamic walking. In: 2016 23rd International Conference on Mechatronics and Machine Vision in Practice (M2VIP); 2016 Nov 28-30; 2016. Nanjing, China. IEEE; 2016. pp. 1-5. DOI
20. Kumar S, Mohammadi A, Quintero D, Rezazadeh S, Gans N, Gregg RD. Extremum seeking control for model-free auto-tuning of powered prosthetic legs. *IEEE Trans Control Syst Technol* 2019;28:2120-35. DOI
21. Krstic M, Wang HH. Stability of extremum seeking feedback for general nonlinear dynamic systems. *Automatica* 2000;36:595-602. DOI
22. Ariyur KB, Krstic M. Real-time optimization by extremum-seeking control. John Wiley & Sons; 2003. DOI
23. Kumar S, Mohammadi A, Gans N, Gregg RD. Automatic tuning of virtual constraint-based control algorithms for powered knee-ankle prostheses. In: 2017 IEEE Conference on Control Technology and Applications (CCTA); 2017 Aug 27-30; Maui, HI, USA. IEEE; 2017. pp. 812-18. DOI
24. Kumar S, Zwall MR, Bolívar-Nieto EA, Gregg RD, Gans N. Extremum seeking control for stiffness auto-tuning of a quasi-passive ankle exoskeleton. *IEEE Robot Autom Lett* 2020;5:4604-11. DOI
25. Morar A. Stepper motor model for dynamic simulation. *Act Electr* 2003;44:117-22. Available from: https://ie.utcluj.ro/files/acta/2003/Number%202/Paper08_Morar.pdf. [Last accessed on 6 March 2024]
26. Choi JY, Krstic M, Ariyur KB, Lee JS. Extremum seeking control for discrete-time systems. *IEEE Trans Autom Control* 2002;47:318-23. DOI
27. Clauser CE, Mc Conville JT, Young JW. Weight, volume, and center of mass of segments of the human body. 1969. Available from: https://ntrs.nasa.gov/api/citations/19700027497/downloads/19700027497.pdf. [Last accessed on 6 March 2024]